JOURNAL OF MATERIALS SCIENCE 18 (1983) 2876–2889

Statistical analysis of multiple fracture in 0°/90°/0° glass fibre/epoxy resin laminates

PETER W. MANDERS*, TSU-WEI CHOU
Department of Mechanical and Aerospace Engineering, University of Delaware, Newark, Delaware 19711, USA

FRANK R. JONES, JOHN W. ROCK
Department of Metallurgy and Materials Technology, University of Surrey, Guildford, Surrey, UK

Measurements of the distributions of crack spacings developed in the 90° ply of 0°/90°/0° glass fibre/epoxy resin laminates under tensile loading show that the ply has a variable strength. As a consequence the strain at which cracking begins is very dependent on the specimen length. The observed distributions of crack spacing are not consistent with the assumption of a uniform strength for the 90° ply. A statistical model provides a good description of the cracking behaviour particularly when the cracks are widely spaced. Magnification of the stress in the matrix between the relatively stiff glass fibres leads to debonding which is observed as a reversible "stress-whitening." The distributions reveal a lower probability of crack formation in the under-stressed region close to the existing cracks and provide estimates of the size of this region. The method of analysis can be applied to many systems which exhibit multiple fracture.

Nomenclature

GBP	Garrett, Bailey, Parvizi
c.d.f.	Cumulative distribution function
i.i.d.	Independent and identically distributed
NMA	Nadic methyl anhydride
BDMA	Benzyl di-methyl amine
A	Cross-sectional area of 90° ply
L	Crack spacing
V	Volume of 90° ply under consideration
b	0° ply thickness
d	90° ply half-thickness
E_0, E_{90}	Young's modulus of 0° and 90° ply, respectively
G_{90}	Shear modulus of 90° ply
y	Distance from plane of crack
N	Total number of crack spacings
n	Subset of N
σ, σ_{90}	Stress, stress in 90° ply
σ_a	Average applied stress on laminate
σ^*, ϵ^*	Weibull scale parameter in terms of stress and strain
w	Weibull shape parameter
β	Exponent in GBP stress function
μ	Average number of cracks per unit length
Γ	Gamma function
S, S_V	c.d.f. for strength of 90° ply, (of volume V)
S_0	c.d.f. for strength of unit volume
R, R_V	Risk of rupture of 90° ply, (of volume V)
ϕ	Risk of rupture per unit volume
u, v, z	Displacement in shear lag analysis
$\Delta\sigma_{90}$	Difference between 90° ply stress in presence of cracks and the expected stress in the absence of cracks
τ	Interfacial shear stress between 0° and 90° plies
$\epsilon_0, \epsilon_{90}, \epsilon_a$	Tensile strains in 0°, 90° plies and applied strain

*Present address: Union Carbide Corporation, Parma Technical Center, 12900 Snow Road, Parma, Ohio 44130, USA.

0022–2461/83 $03.00 + .12
© *1983 Chapman and Hall Ltd.*

1. Introduction

Although unidirectionally reinforced fibre composites can offer extremely high specific strength and stiffness in the fibre direction, their strength under off-axis loading is generally rather poor and many practical applications call for a proportion of the fibres to be orientated so as to support these loads. For example, a pressurized cylinder might have fibres placed at right angles so as to take the longitudinal and hoop loads. Biaxial stress states such as this, in which the stress ratio and directions are fixed, lend themselves to a 0°/90° arrangement of fibres along the principal axes. More elaborate configurations of fibres are required for more complex states of stress, but the principles discussed here can still be applied.

Composites reinforced with fibres in the 0° and 90° directions are typically fabricated from pre-impregnated sheets of fibre (pre-preg), by filament winding and braiding, or from woven cloth. All of these give rise to structures in which there are discrete layers of fibre. In filament-wound, woven and braided structures the sequence of fibre orientations varies from place to place, but they exhibit similar micro-cracking phenomena to the laminates discussed here.

The strain at which failure occurs perpendicular to the fibres is generally less than in the direction of the fibres, and when the composite is strained beyond this point a network of cracks develops in the 90° ply. This phenomenon is illustrated for 0°/90°/0° laminates by Fig. 1, and has been extensively studied by many workers [1–15]. As the strain is increased the crack spacing decreases and ultimately sufficiently high stress may be generated in the longitudinal 0° plies by Poisson contraction to cause cracking in these too, Figs. 1e to i and r as noted by Bailey *et al.* [5] and Aveston and Kelly [10].

Multiple cracking

(i) reduces the effective stiffness of the 90° ply leading to redistribution of load within the structure,

(ii) allows fluid weepage,

(iii) allows the ingress of moisture or other detrimental (particularly corrosive) fluids,

(iv) may lead to delamination between the plies [12–15], and

(v) modifies the effective toughness of the laminate.

It is therefore important to know at what strain cracking will occur and what the spacing will be.

Garrett, Bailey and Parvizi (GBP) accounted for the increasing density of cracks with strain in terms of the non-uniform redistribution of load between the plies in 0°/90°/0° glass fibre/resin matrix laminates [1–5, 7]. This increase might also be explained in terms of a distribution of defects in the ply which propagate over a range of applied load to form the cracks.

Parvizi *et al.* [3] also showed that the strain at which multiple cracking begins is higher when the thickness of the 90° ply is less and they explained this in terms of the energetics of the fracture process. Their argument follows that of Aveston and Kelly [8] and Aveston *et al.* [9] and defines a lower bound on the failure stress which is based on the thermodynamic requirement that the release of stored energy accompanying the formation of a crack must equal or exceed the energy of formation of the new fracture surfaces. The analysis [3] did not consider the mechanism by which a crack grew, but this has been done by the fracture mechanics approach developed by Wang and co-workers [11–15] employing finite element methods to obtain the energy release rate. The principle of both approaches is that the crack surface energy requirement decreases linearly with ply thickness, whereas the energy release decreases faster. Crack formation can therefore be inhibited by decreasing the ply thickness and this is termed "constraint." A higher applied strain is then required to make fracture possible.

In this paper we show that the deterministic multiple cracking theory of GBP cannot fully account for the measured distribution of crack spacings and we propose a simple statistical model which accurately fits the data and predicts a dependence of strength on size. We discuss the origins and implications of this variability of strength, and analyse the results so as to obtain its approximate magnitude. The method of analysis can be applied to many systems which exhibit multiple fracture, for example surface coatings, oxide layers, fibres or matrix in unidirectional composites and hybrid composites.

2. Experimental procedure

2.1. Fabrication

Three-ply laminates were prepared by winding tows of Silenka E-glass fibre onto frames which were stacked in a 0°/90°/0° sequence and then vacuum impregnated with an Epikote 828/NMA/BDMA (100:80:1.5) epoxy resin system. The impreg-

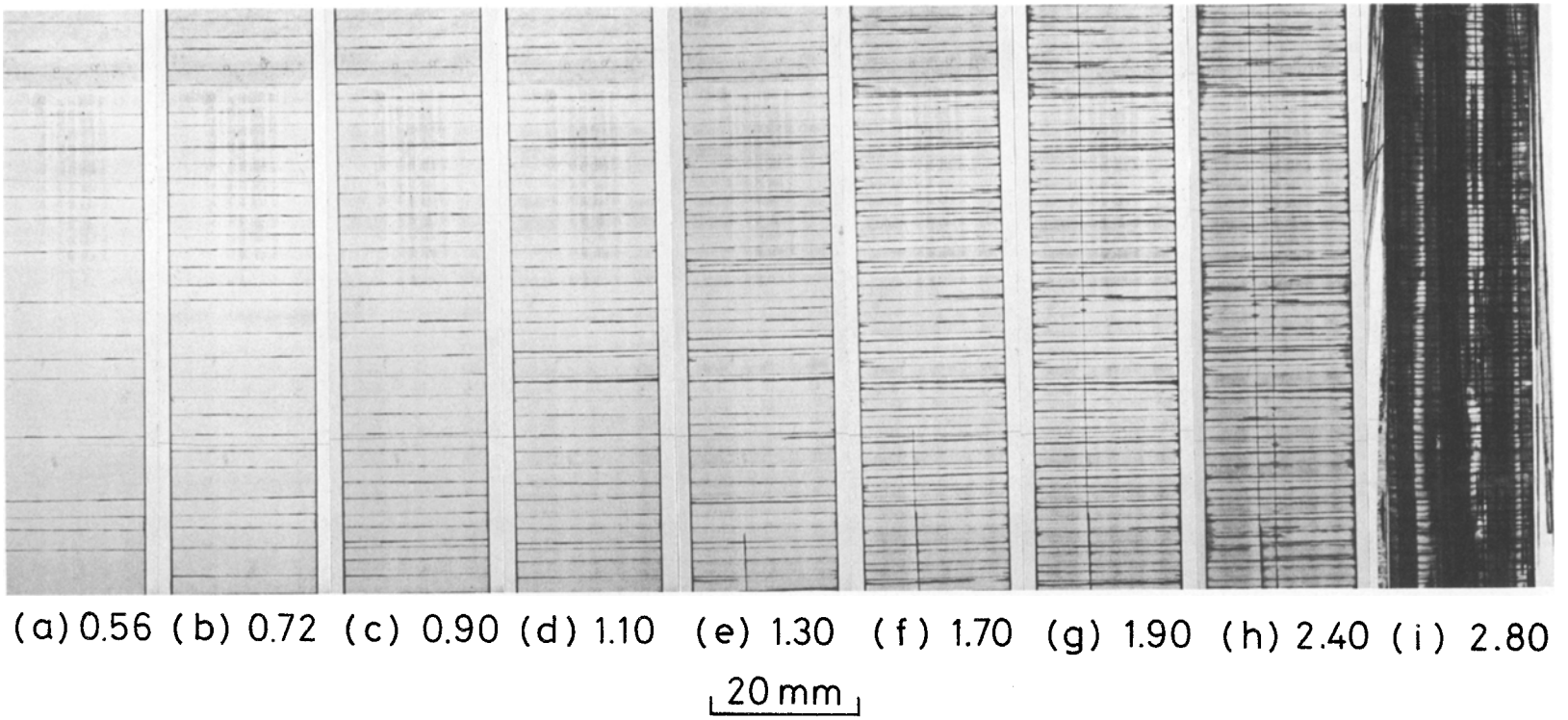

Figure 1 Photographs of specimens at the indicated strain levels (%) under (a to i) bright field, and (j to r) dark field illumination. Note: multiple transverse cracks in the 90° ply, stress "whitening" and longitudinal splitting in the 0° plies.

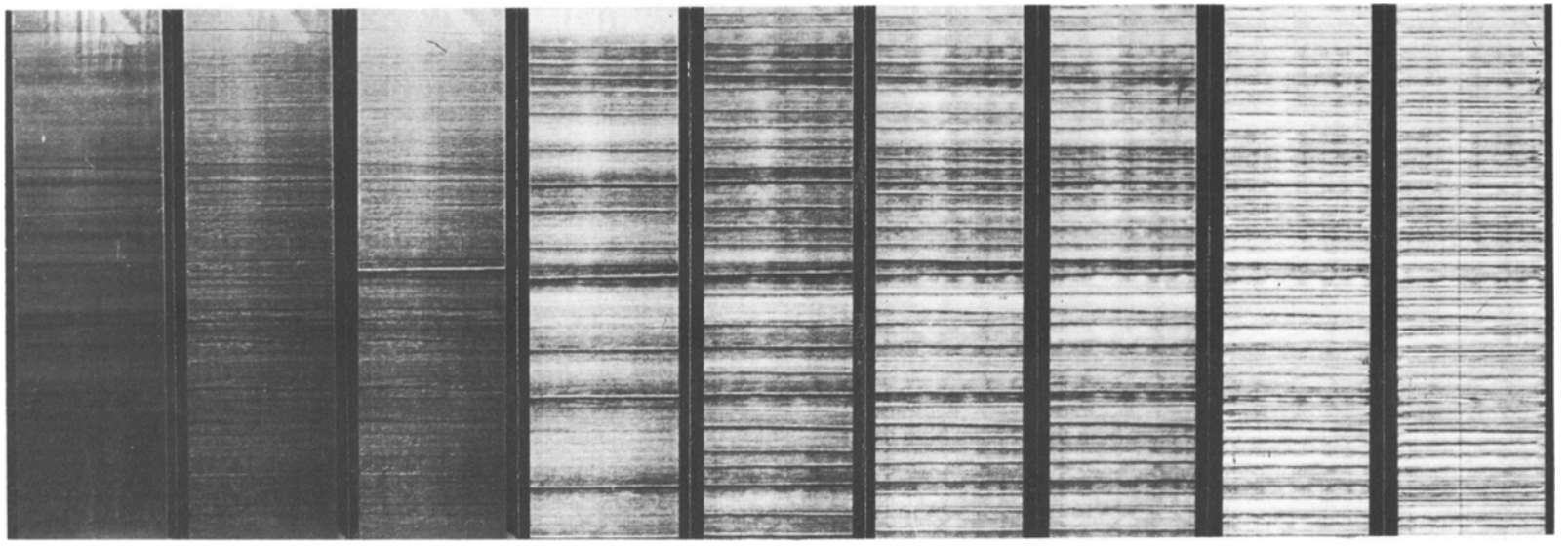

Figure 1 Continued.

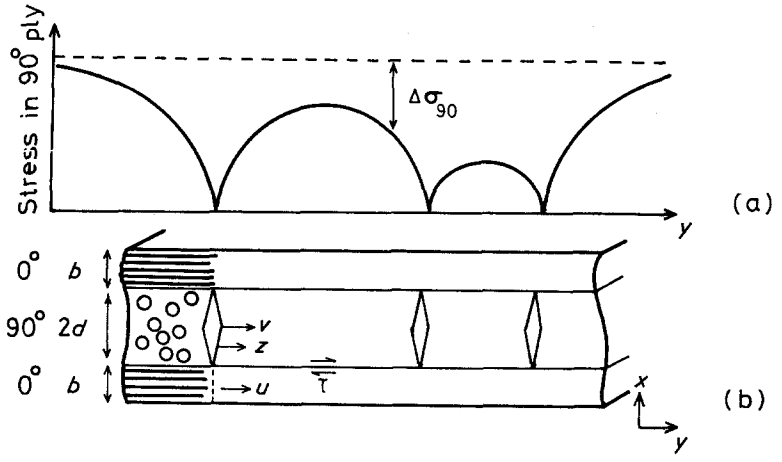

Figure 2 (a) Schematic diagram of the tensile stress in the 90° ply. If the cracks were not present it would be as indicated by the dashed line. (b) Cross-section of laminate corresponding to (a) showing the displacements used in the shear-lag analysis.

nated lay-ups were cured between plates under a pressure of 3 kPa for 3 h at 100° C and postcured for 3 h at 150° C in an air-circulation oven to obtain void-free laminates of about 50% volume fraction. The central 90° ply was 1.1 mm thick and was sandwiched between two 0.55 mm plies in the symmetric sequence shown in Fig. 2. A close match between the refractive indices of the fibre and matrix made the laminates virtually transparent so that cracking and microscopic damage in the 90° ply could be closely observed, Fig. 1. The laminates were cut into parallel-sided test pieces with a 600 grit diamond saw and were tested in tension.

2.2. Observation of cracking

The pattern of cracks was photographed at regular intervals of applied load using either bright- or dark-field illumination. Dark-field illumination, Fig. 3a, showed fibre–matrix debonding ("stress whitening" which scattered light) with good contrast, Fig. 1j to r, whereas bright-field illumination Fig. 3b gave better definition of the cracks, Fig. 1a to i, although in this case the fibre–matrix debonding appeared dark with rather poor contrast.

2.3. Measurement of thermal strain

In cooling from the postcure temperature of 150° C to ambient the 90° ply was placed under

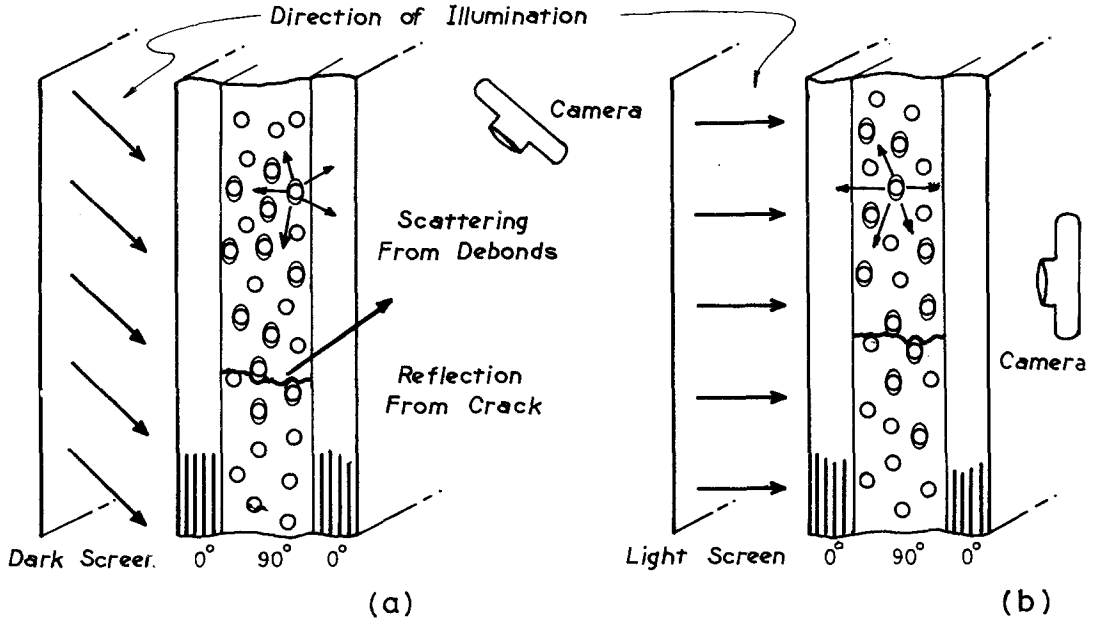

Figure 3 Illumination of laminates for photography. (a) Dark field which shows transverse cracks and debonding as light on a dark background. (b) Bright field in which contrast is reversed.

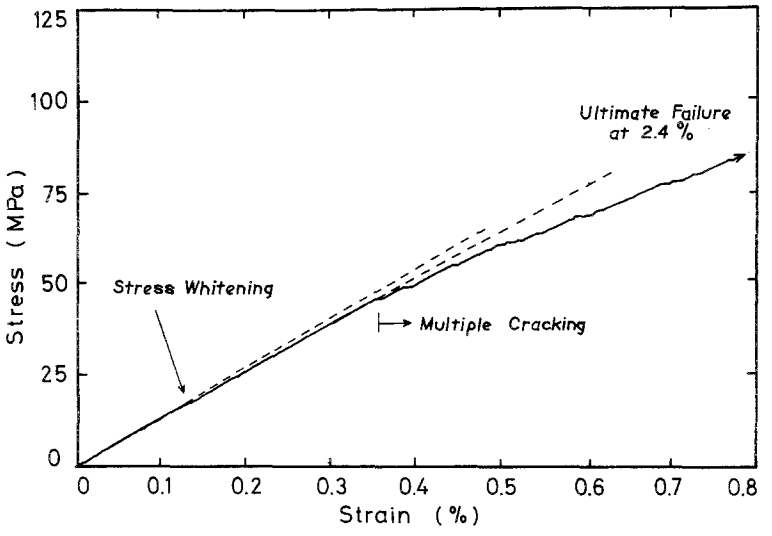

Figure 4 Low strain portion of stress/strain curve. Changes of gradient are associated with a rapid increase in stress whitening, and with the beginning of multiple cracking.

0.22% tensile strain with respect to the 0° plies on account of its higher coefficient of thermal expansion. This thermal strain was assessed from the bending of unbalanced 0°/90° beams rather than from expansion coefficients since this eliminates errors arising from uncertainty about the temperature at which the strains were effectively frozen in.

3. Results

3.1. Description of loading

Even in the absence of applied load the dark-field technique of illumination showed up striations along the fibres in fibre-rich regions and from this we infer that limited fibre/matrix debonding occurs under the residual thermal stress. Bailey and Parvizi [6] have shown that such debonding occurs under the residual stresses existing in glass fibre/polyester 0°/90°/0° laminates but suggested that it did not occur in the case of glass fibre/epoxy resin laminates of similar geometry to those discussed here. We suggest that this is a question of degree and that the dark-field illumination is a more sensitive technique for detecting initial debonding.

As the specimens were loaded the initial whitening progressively increased, most noticeably at about 0.34% strain Fig. 1k. A knee visible in the stress/strain curve, Fig. 4, at approximately 0.1% can be identified with a similar knee observed by Bailey and Parvizi [6], who interpreted this as the strain at which fibre/matrix debonding began.

Cracks appeared instantaneously at about 0.4% strain, often, but not exclusively, in the bands of more pronounced whitening Figs. 1*l* and m. It is apparent from this, and microscopic observations [6], that a crack forms by the joining up of the fibre–matrix debonds. The beginning of multiple cracking caused a second knee in the stress/strain curve and a progressive loss of stiffness thereafter, Fig. 4. Note that the stress whitening diminished in intensity for a distance approximately equal to the ply thickness on either side of a crack, Fig. 1. We attribute this reverse to the relaxation of stress in the 90° ply in the vicinity of the crack which allows the debonds to close up. Reversibility of stress whitening on relief of load was observed by Parvizi [6] and was correlated with closure of debonds by *in situ* electron microscopy. As the load was further increased the whitening in all areas intensified, but in the regions close to the cracks it never equalled the intensity developed further away from cracks.

The rate of crack formation with applied strain decreased throughout the loading. At higher strains the crack spacing became more uniform and is discussed in Section 3.2. At a strain of about 0.7% stress whitening appeared in the longitudinal 0° ply, Fig. 1n to r (seen as darkening in Fig. 1b to i) and this developed into longitudinal cracks at about 1.8% strain (also accompanied by relief of the whitening). This occurs because the 0° plies are placed in transverse tension as a result of their Poisson contraction being restrained by the 90° ply as described by Bailey *et al.* [5].

3.2. Distribution of crack spacings

The positions of every crack in a photograph of the highest load case were measured by travelling microscope and the crack positions for lower loads

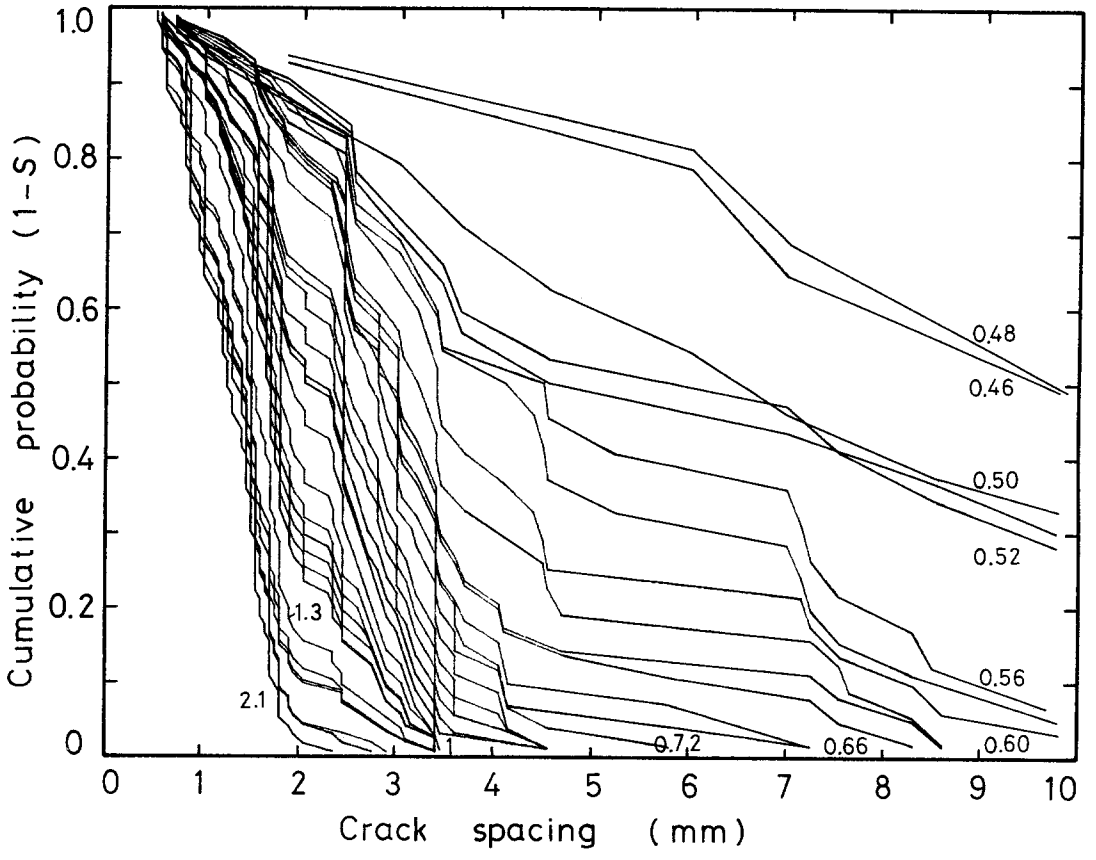

Figure 5 Distributions of crack spacings measured at the indicated levels of applied strain (%). Intermediate strains may be found from the solid circles in Fig. 9.

were inferred by noting which were not present. A computer program calculated the spacings between cracks and their cumulative distribution functions (c.d.f.'s) for each load case (shown in Fig. 5) which give the probability (S) that the distance between two cracks is less than some specified value. While these distributions illustrate the overall trend towards closer spacings at higher strains, they also embody a great deal more information which is discussed in Section 4. In particular, it should be noted that there are very few crack spacings less than about 1 mm.

4. Discussion

4.1. Strength of the 90° ply

In resin matrix composites, the 90° ply invariably fails at a lower strain than the 0° plies because

(i) the matrix is inherently weaker than the fibres, and

(ii) there is a magnification of stress in the matrix between the relatively stiff fibres as shown by Kies [16].

Because the fibres are packed randomly there is a random distribution of this stress magnification factor, and even in the absence of other sources of variability the strength of the 90° ply will vary from place to place. Ignoring any tendency for the fibres to remain clumped in their tows, we expect the strength of the 90° ply to be statistically the same throughout its volume, i.e. constituent volumes which are substantially larger than the microstructure should have strengths which are independent of each other and which are identically distributed (i.i.d.).

4.2. Distribution of crack spacings

The cracks appear at the weakest cross-sections of the 90° ply with some mean frequency (density) along the length which depends on the applied strain. If it is assumed that the strengths of successive-sections are i.i.d., this will be a Poisson process, from which it can be shown (see standard probability text) that the intervals between adjacent cracks will be exponentially distributed with cumulative probability

$$(1 - S) = \exp(-\mu L) \quad (1)$$

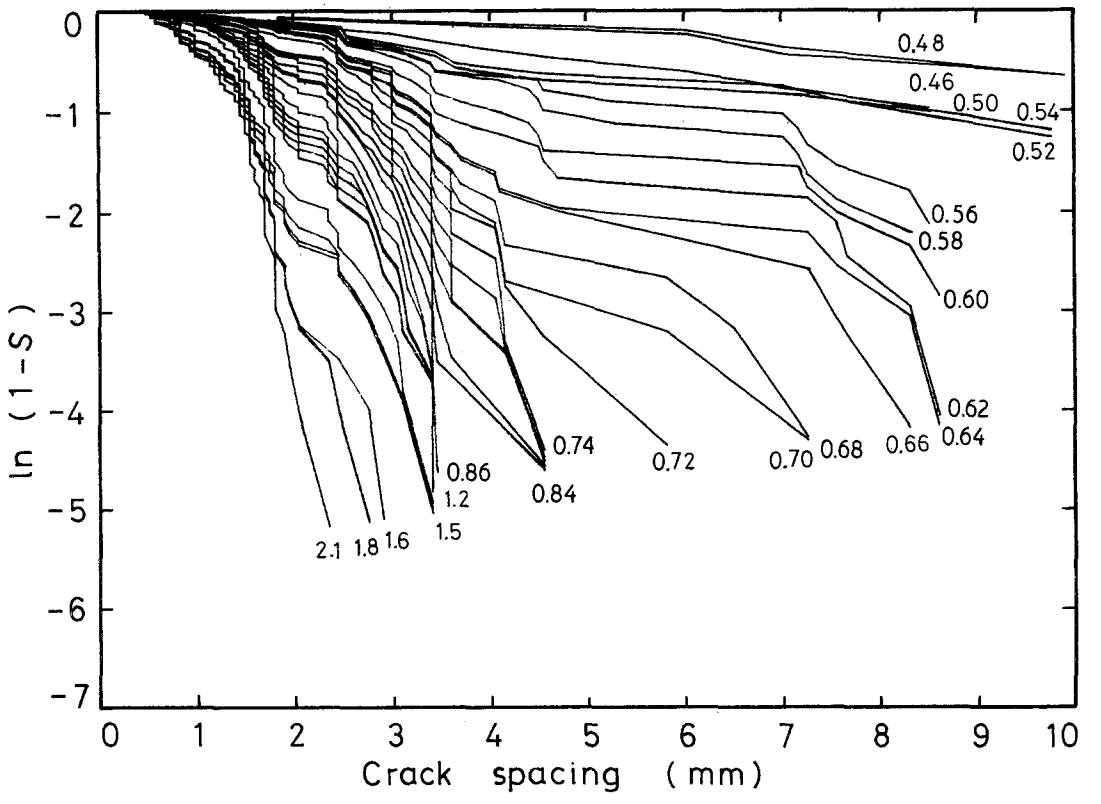

Figure 6 Distributions of crack spacings from Fig. 5 plotted on logarithmic probability axis. Note positive intercepts on crack spacing axis, and their relative linearity above approximately 2 mm.

where μ is the mean crack density and L is length.

This is easily tested. Taking logarithms

$$\ln (1 - S) = -\mu L \qquad (2)$$

it is seen that a graph of $\ln(1-S)$ against crack spacing L should be linear with a gradient $-\mu$ and should pass through the origin. The value of μ depends upon the level to which the ply was stressed and the strength distribution about which we have so far made no assumption. However, the curves in Fig. 6 are clearly not perfectly linear, nor do they pass through the origin. They are more linear at larger crack spacings (and lower stresses) where they follow Equations 1 and 2 more closely, and this shows that the probability of cracking rises, and becomes nearly constant (as expected from the assumption of i.i.d. strengths on each cross-section), away from existing cracks. All curves appear to meet the L axis asymptotically at the origin. Straight lines have been least squares fitted to the linear portions of these curves in order to obtain the intercept on the crack spacing axis. The intercept represents the distance either side of a crack in which the probability of another crack forming is effectively zero, and it is plotted against the applied strain (not corrected for residual thermal strains) in Fig. 7. This effectively "unstressed" length decreases from slightly above to slightly below the 90° ply thickness (1.1 mm) as the applied strain increases. The probability of cracking is depressed close to existing cracks because the stress is lower, actually zero in the plane of the crack. The load in the 90° ply builds up to either side of a crack by shear stress transfer from the 0° plies.

Fig. 2 shows that the maximum tensile stress (and strain) in the 90° ply occurs midway between two cracks, but that it is less than that existing just before the cracks formed, or far removed from the cracks. The GBP model's assumption of uniform strength in the 90° ply therefore leads to the prediction that the next crack should always form midway between the two most widely spaced cracks. Although the initial crack in a given gauge length occurs at random, the positions of subsequent cracks are fully determined. Whatever the position of the first crack the ratio of maximum to minimum crack spacing cannot exceed 2 in the

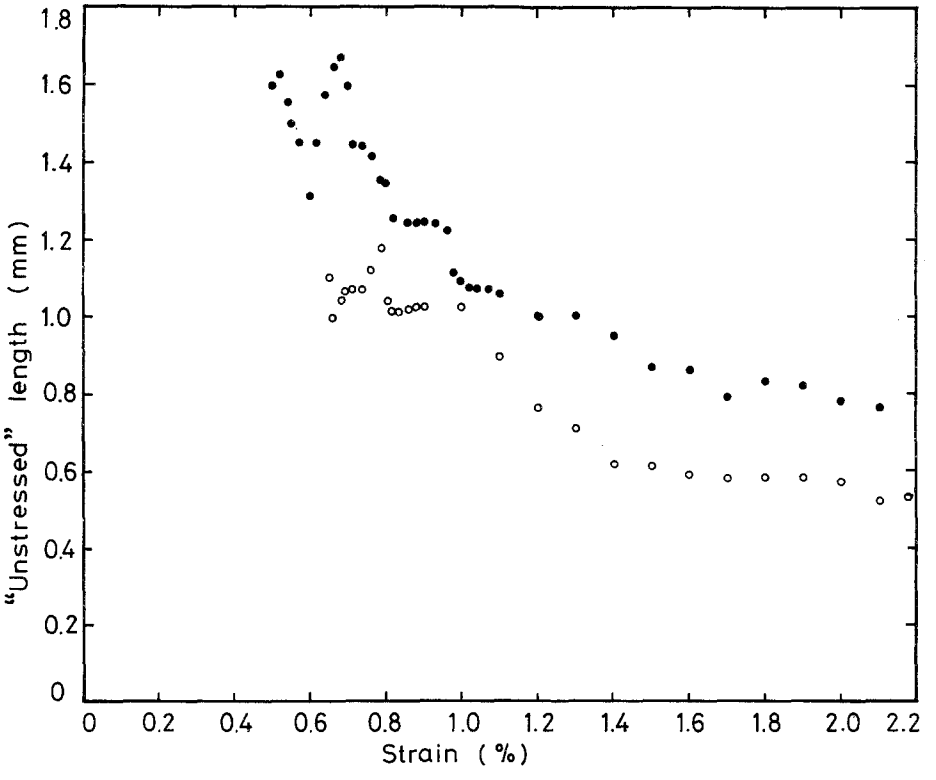

Figure 7 Variation of "unstressed length" (crack spacing intercept from Fig. 6) with applied strain. (Two nominally identical specimens.)

GBP model. However, the experimental crack spacing c.d.f.'s in Fig. 5 shows that this factor of 2 is greatly exceeded particularly at low strain and that the fixed-strength model is inadequate in this region.

The GBP model calculated the additional stress that had to be applied to the laminate to raise the maximum stress between the two most widely spaced cracks to the value at which another crack would form, and thereby obtained bounds on the crack density as a function of applied stress, geometrical factors, and stiffness of the plies. Since the assumption of a unique 90° ply cracking strain has been shown to be unrealistic we suggest that a statistical description of the crack spacing is more appropriate at low strains where the cracks are widely spaced.

4.3. Variation of crack spacing with stress

We assume that the 90° ply is an ideal homogeneous brittle material with an inherent distribution of strength which is described by a c.d.f. termed S_0 for failure of a unit volume. Assuming also that the strengths of all the constituent volumes are i.i.d., the c.d.f. of strength S_V for a volume V under uniform stress is given by

$$(1-S_V) = (1-S_0)^V \tag{3}$$

because no sub-volume may fail if the volume V as a whole is not to fail. Taking logarithms gives

$$\ln(1-S_V) = V\ln(1-S_0) = -R_V \tag{4}$$

where R_V is termed the "risk of rupture" by Weibull [17, 18] and depends on volume and stress or strain. Writing

$$\ln(1-S_0) = -\phi(\sigma) \tag{5}$$

we have a risk of rupture dR for a volume element dV

$$dR = -\ln(1-S_0)\,dV = \phi(\sigma)\,dV. \tag{6}$$

For a non-uniform state of stress the risk of rupture for a volume V is given by

$$R_V = \int_V \phi(\sigma)\,dV \tag{7}$$

and its c.d.f. for failure is then

$$S_V = 1-\exp(-R_V) = 1-\exp\left[-\int_V \phi(\sigma)\,dV\right]. \tag{8}$$

Since the stress is assumed to be uniform through the width and thickness the volume integral may be replaced with an integration over length.

$$S_V = 1 - \exp\left[-A\int_L \phi(\sigma)\,dy\right]. \quad (9)$$

This integral equation could be solved by curve fitting to the measured distributions in order to obtain both the variation of stress between cracks and the dependence of the probability of failure on stress. However, a solution of this type would not be in closed analytical form and involves some practical difficulties. Instead, our approach is to extract only information about the variability of the strength of the ply.

In the Appendix we propose a shear-lag solution for the stress between cracks and show how this can be combined with a statistical description of the non-uniformity of strength. However, there are considerable difficulties in obtaining a solution which gives the crack spacing in terms of the applied stress or strain. At low strains the cracks are widely spaced and the GBP model is less accurate because the stress between cracks is relatively uniform and the crack positions are principally determined by the weak points in the 90° ply. The next section shows how a simple model based on a fitted Weibull distribution accurately describes the crack spacings under these conditions.

When the cracks are widely spaced the integral in Equation 9 may be approximated, as below, by assuming a constant level of stress between cracks. Taking logarithms gives

$$\ln(1 - S_V) = -A\int_L \phi(\sigma)\,dy \approx -A\phi(\sigma)L. \quad (10)$$

The quantity $A\phi$ is found from the gradient when $\ln(1 - S_V)$ is plotted against L as in Fig. 6.

A two-parameter Weibull distribution [17, 18] is assumed for the strength of the 90° ply in which

$$A\phi = A\left(\frac{\sigma}{\sigma^*}\right)^w = A\left(\frac{\epsilon}{\epsilon^*}\right)^w. \quad (11)$$

The constants σ^* and ϵ^* are the scale parameters in terms of stress and strain, respectively, and w is the shape parameter (an inverse measure of the variability). Taking logarithms of Equation 11 gives

$$\ln(A\phi) = w\ln\epsilon - w\ln\epsilon^* + \ln A \quad (12)$$

from which it is seen that a graph of the logarithm of the gradients obtained from Fig. 6 plotted against the applied strain (after correction for residual thermal strain) will be linear with gradient w if the Weibull distribution is valid. This has been done in Fig. 8 in which there are two linear regions intersecting at a strain of about 0.4% (corrected for residual thermal strain), or 0.6% applied strain. At low strain, w is about 8.5 and about 1.0 at high strain. This change in gradient indicates that the strength of the 90° ply becomes effectively more variable at higher strains. The two intercepts ($\ln A - w\ln\epsilon^*$) corresponding to the two linear segments are 47 and 11 (strain and length in fundamental units). Working in terms of strain one assumes that the laminate has a linear-elastic response even after cracking. This has been done because the moduli of the individual plies in the particular laminates were not measured and thermal strain correction can be made more accurately as a strain. For relatively large crack spacings where the statistical model is most appropriate this approximation leads to minimal error.

Equation 10 has been evaluated after substitution of Equation 11 using the fitted values of $w = 8.5$ and intercept = 47 in order to obtain median crack spacings ($S_V = 0.5$) as a function of strain. A constant value of unstressed length of 1.3 mm taken from Fig. 7 was added to the median crack spacing before calculating the expected crack spacing. This is plotted as the solid curve in Fig. 9 after allowing for the residual tensile thermal strain, and is seen to be a good description of a wide range (2 to 50 mm) of crack spacing particularly since the "unstressed length" has been assumed to be constant. Although the simple statistical model relies on fitting to experimental measurements of variability it offers two significant improvements over the GBP model. It accurately describes the distribution which contains both widely- and closely-spaced cracks at low strains, and it predicts that the strain at which a crack first appears depends on the length of the specimen as discussed in the next section.

The GBP and probabilistic models are complementary. At low strains, the crack spacing is large and the length required to build up stress in the 90° ply either side of a crack is small in comparison. Therefore most of the region between cracks is relatively uniformly stressed and the positions of new cracks are determined principally by the distribution of weak points. Only rarely does a new

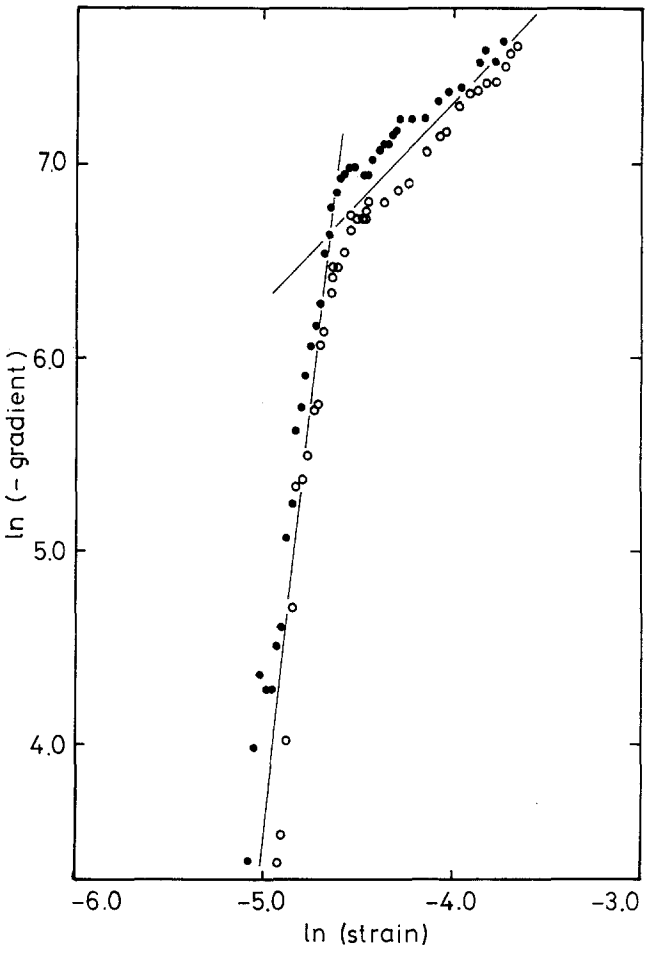

Figure 8 Variation of gradients from Fig. 6 (see text) with 90° ply strain, corrected for residual thermal strain.

crack form exactly midway between two existing cracks and this is why the distribution of crack spacings covers a wider range than the factor of two predicted by the GBP model. Therefore at low strains the probabilistic model is more appropriate.

At high strains the opposite is true. The region between cracks is very non-uniformly stressed and since the highest stress in the 90° ply is found midway between existing cracks this is where the new cracks form as described by the GBP model. When the crack spacing is significantly larger than the unstressed length (approximately 1.3 mm for the laminates described here) the probabilistic model is appropriate, and when it is of similar magnitude the GBP model is more appropriate.

4.4. Size dependence of cracking strain

The coefficient of variation of the Weibull distribution is given by

$$\left[\frac{\Gamma(1+2/w)}{\Gamma^2(1+1/w)}-1\right]^{1/2} \qquad (13)$$

so that the value of $w = 8.5$ at low strains corresponds to a coefficient of variation for the failure strain of the 90° ply of about 14% when referred to the actual strain in the 90° ply. The coefficient of variation is about 24% when referred to the applied strain (which is lower than the actual strain by the residual thermal strain). However it must be realized that this estimate of variability is based on an approximate Weibull shape parameter which has been fitted to data in the range 0.5 to 1.0% strain. Because the variability effectively increases with strain (w decreases, Fig. 8) the estimate can be expected to be somewhat above the coefficient of variation of the first cracking strain and indeed this is so.

However any degree of variability leads to a size effect in which the failure strain of the 90° ply increases as its length is decreased. From Equation 10 (after substitution of Equation 11) it is seen that the ratio of failure strains is $1/w$ of the ratio of lengths, in the case of the laminates described here about 0.12.

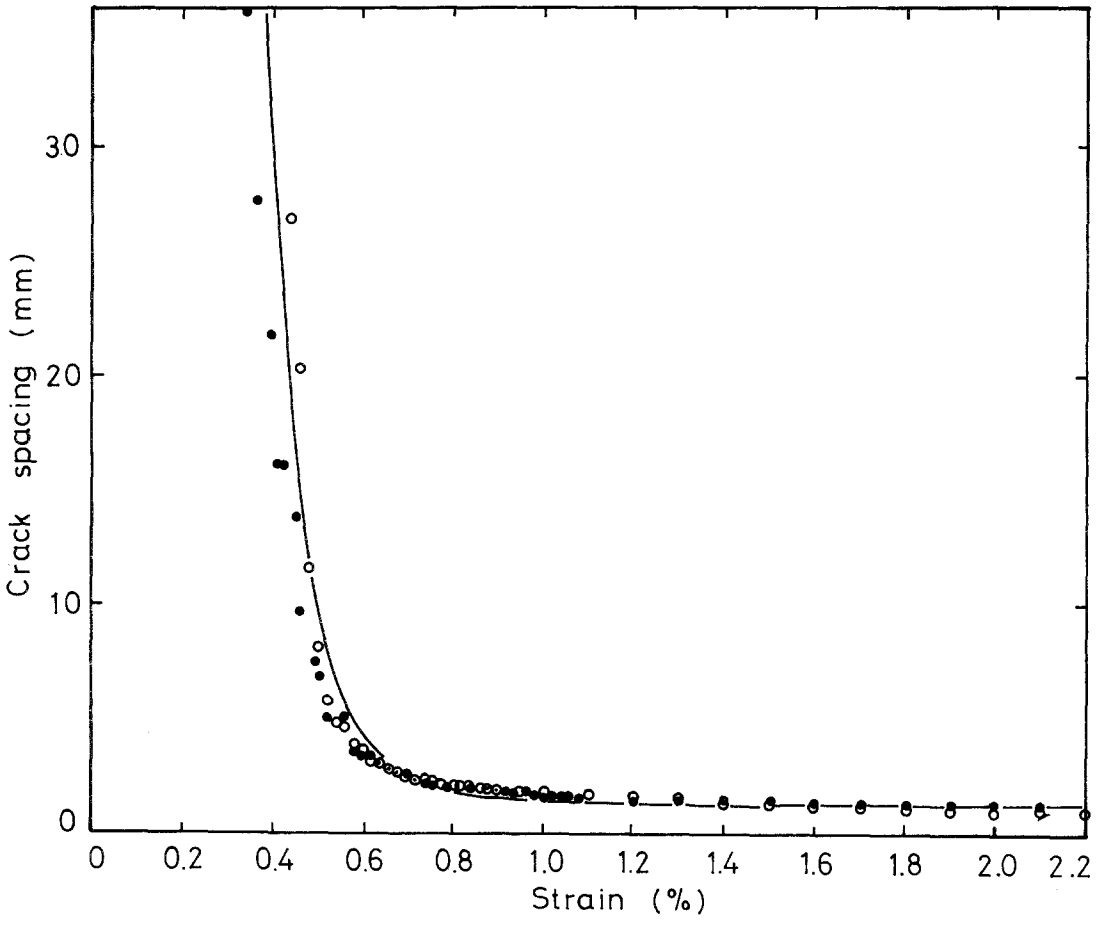

Figure 9 Crack spacing as a function of strain. Solid and open circles correspond to two nominally identical specimens. Solid curve is derived from statistical model – see text.

This is an important consideration because the first transverse cracking strain which is commonly measured and discussed [5, 10] depends on the length of the specimen tested. Similarly the first crack will appear at lower strains in wider and/or thicker 90° plies if the cracks initiate randomly throughout the volume of the 90° ply. Such an effect has been found for changes in thickness and has previously been explained in terms of fracture energetics [3] although statistical size effects were not considered. Any fracture process is ultimately governed by thermodynamic considerations, but from a practical point of view, these may be dominated by the variability arising from the randomness of the microstructures.

It is probable that most transverse cracks initiate at the cut edge of the specimen and not randomly throughout the volume. In this case there should be identical size effects for changes in length and thickness since both of these affect the area of cut edge equally, but no size effect for changes in width. Tubular (e.g. filament-wound) structures without cut edges could behave very differently from cut specimens. If the area of the cut edge is the dominant factor, not volume, then the above analysis should be modified by replacing length and volume by area of edge in the integration in Equation 10, and in Equations 3 to 10.

It would be most interesting to know how the variability of the 90° ply strength depends on the fibre volume fraction, fibre/matrix bond strength and fibre shape and size, in order to assess the relative importance of geometrical factors and materials properties. In the particular case of carbon fibre/epoxy resin composites the fibres themselves are known to fracture on occasion before the fibre/matrix bond [5] and if this determines the strength of the 90° ply, it might give rise to a different variability from that of glass fibre composites.

The debonding between fibre and matrix is arrested by energetic factors at an intermediate

stage of crack formation. These debonds then coalesce to form a macroscopic crack in a process which is dominated by the random nature of the microcracked structure. Both processes are linked by the stress distribution around a crack. (The reversal of stress whitening for roughly one ply thickness either side of a crack in accordance with Equation 3 is evidence of this.) The processes occurring at the fibre/matrix interface which allow debonding to be reversed with relief of stress and thermal annealing [6] are presently unknown, but deserve greater attention because they determine the statistical properties of the material in which a crack ultimately forms.

5. Conclusions

Measurements of the distributions of crack spacings in 0°/90°/0° glass fibre/epoxy resin laminates have shown that a model based on a unique value of strength for the 90° ply is unable to account for the spacings. The statistical variability of the 90° ply strength must therefore be considered and a model incorporating a Weibull distribution of strength is shown to be a good description of the crack spacings.

This variability leads to a size effect in which the first crack appears at a strain which increases as the length of the specimen is decreased. The measured distributions of crack spacings indicate an intrinsic coefficient of variation (in the absence of residual strains) for the failure strain of the 90° ply of about 14% and this is attributed to the stress magnifications arising from random packing of the fibres.

Fibre/matrix debonding causes "stress whitening" which is reversible and indicates the approximate distribution of stress in the 90° ply.

Acknowledgements

We are grateful to the Science and Engineering Research Council for a research studentship (J.W.R.) and an equipment grant. We would all like to thank Professor J. E. Bailey, Dr A. Parvizi Majidi, Mr M. G. Bader and Dr K. Aderogba for discussion and comments on the work and Mr D. H. Jeske and Mr Q. P. V. Fontana for technical assistance. This work has been partially supported by the United States Department of Energy under contract number DE-AC01-79ER10511.

Appendix

The shear-lag analysis gives the tensile stress in the 90° ply between two cracks spaced L apart and is based on the same assumptions of elastic continuity and uniformity of deformations as the analysis of Garrett and Bailey [1]. The displacements which are functions of y are illustrated in Fig. 2b.

The displacement of the 0° ply is assumed to be uniform through its thickness while the displacement of the less stiff 90° ply increases towards the mid-plane. The interfacial shear stress is given by

$$\tau = \frac{(v-u)}{d} G_{90}. \tag{A1}$$

By force equilibrium

$$\frac{\mathrm{d}\Delta\sigma_{90}}{\mathrm{d}y} = \frac{(u-v)}{d^2} G_{90} \tag{A2}$$

where $\Delta\sigma_{90}$ is the difference between the 90° ply stress at position y and its value in the absence of cracks $\epsilon_a E_{90}$. Differentiating with respect to y

$$\frac{\mathrm{d}^2\Delta\sigma_{90}}{\mathrm{d}y^2} = \frac{G_{90}}{d^2}\left(\frac{\mathrm{d}u}{\mathrm{d}y} - \frac{\mathrm{d}v}{\mathrm{d}y}\right) = \frac{G_{90}}{d^2}(\epsilon_0 - \bar{\epsilon}_{90}) \tag{A3}$$

assuming that

$$\frac{\mathrm{d}v}{\mathrm{d}y} = \frac{\mathrm{d}\bar{v}}{\mathrm{d}y} = \bar{\epsilon}_{90}. \tag{A4}$$

A force balance gives

$$\epsilon_{90} = \left(\epsilon_a - \frac{\Delta\sigma_{90}}{E_{90}}\right) \tag{A5}$$

and

$$\epsilon_0 = \left(\epsilon_a + \frac{\Delta\sigma_{90}}{E_{90}}\frac{d}{b}\right). \tag{A6}$$

Substitution into Equation A3 gives

$$\frac{\mathrm{d}^2\Delta\sigma_{90}}{\mathrm{d}y^2} = \beta\Delta\sigma_{90} \tag{A7}$$

where

$$\beta = G_{90}\left(\frac{1}{E_0 bd} + \frac{1}{E_{90}d^2}\right). \tag{A8}$$

The general solution to this equation is

$$\Delta\sigma_{90} = X\exp(-\beta^{1/2}y) + Y\exp(\beta^{1/2}y). \tag{A9}$$

X and Y are evaluated for a length of 90° ply bounded by cracks at $y = 0$ and $y = L$ where $\Delta\sigma_{90} = \epsilon_a E_{90}$ (there is no tensile force across the crack faces)

$$X = \frac{\epsilon_a E_{90}[\exp(\beta^{1/2}L) - 1]}{\exp(\beta^{1/2}L) - \exp(-\beta^{1/2}L)} \tag{A10}$$

$$Y = \frac{\epsilon_a E_{90}[1 - \exp(-\beta^{1/2}L)]}{\exp(\beta^{1/2}L) - \exp(-\beta^{1/2}L)}. \quad \text{(A11)}$$

The analysis differs from [1] in that substitution of Equations A10 and A11 into Equation A9 gives $\Delta\sigma_{90}$ directly.

This shear-lag analysis can be incorporated into the statistical description of crack spacings by obtaining

$$\epsilon_{90} = \epsilon_a - \frac{\Delta\sigma_{90}}{E_{90}} \quad \text{(A12)}$$

and substituting into Equation 9

$$S_V = 1 - \exp\left\{-\frac{A}{\epsilon^{*w}}\int_0^L \left[\epsilon_a - \frac{X}{E_{90}}\exp(-\beta^{1/2}y) - \frac{Y}{E_{90}}\exp(\beta^{1/2}y)\right]^w dy\right\}. \quad \text{(A13)}$$

Numerical methods are needed to solve this integral equation for the crack length corresponding to any desired probability level (e.g. 0.5 for median spacing) and are not attempted in this paper.

References

1. K. W. GARRETT and J. E. BAILEY, *J. Mater. Sci.* **12** (1977) 157.
2. *Idem, ibid.* **12** (1977) 2189.
3. A. PARVIZI, K. W. GARRETT and J. E. BAILEY, *ibid.* **13** (1978) 195.
4. A. PARVIZI and J. E. BAILEY, *ibid.* **13** (1978) 2131.
5. J. E. BAILEY, P. T. CURTIS and A. PARVIZI, *Proc. Roy. Soc. Lond.* **A366** (1979) 599.
6. J. E. BAILEY and A. PARVIZI, *J. Mater. Sci.* **16** (1981) 649.
7. A. PARVIZI, PhD thesis, University of Surrey, UK (1978).
8. J. AVESTON and A. KELLY, *J. Mater. Sci.* 8 (1973) 352.
9. J. AVESTON, G. A. COOPER and A. KELLY, Proceedings of National Physical Laboratory Conference "The Properties of Fibre Composites" National Physical Laboratory, UK, November 1971 (IPC Science and Technology Press Ltd, 1971) pp. 15–26.
10. J. AVESTON and A. KELLY, *Phil. Trans. Roy. Soc. Lond.* **A296** (1980) 519.
11. A. S. D. WANG, C. E. LAW and W. J. WARREN, in "Modern Developments in Composite Materials and Structures", edited by J. R. Vinson (ASME, New York, 1979).
12. A. S. D. WANG and F. W. CROSSMAN, *J. Composite Mater.* Supplemental Volume (1980) 71.
13. F. W. CROSSMAN, W. J. WARREN, A. S. D. WANG and G. E. LAW Jr, *ibid.* Supplemental Volume (1980) 88.
14. A. S. D. WANG, 3rd International Conference on Composite Materials, Paris, August 1980. Published in "Advances in Composite Materials", Vol. 1 (Pergamon, Oxford, 1980) pp. 170–182.
15. F. W. CROSSMAN and A. S. D. WANG, ASTM Symposium on Damages in Composite Materials: Basic Mechanisms, Accumulation, Tolerance, and Characterization, Bal Harbour, Florida, November 1980, edited by K. L. Reifsnider, ASTM STP 775 (ASTM, Philadelphia, 1982).
16. J. A. KIES, US Naval Research Laboratory, Report No. 5752 (1962).
17. W. WEIBULL, *Ing. Vetenskapsakad. Handl. Nr.* **151** (1939).
18. *Idem, ibid.* **153** (1939) 1.

Received 20 September 1982
and accepted 18 February 1983